Research Article Vol. 30, No. 5 / 28 Feb 2022 / Optics Express 8063
Optics EXPRESS

Effective Michelson interference observed in fiber-optical analogue of Hawking radiation

RODRIGO FELIPE-ELIZARRARAS,[1] HECTOR CRUZ-RAMIREZ,[2] KARINA GARAY-PALMETT,[3] ALFRED B. U'REN,[2] AND DAVID BERMUDEZ[1,*]

[1]Departamento de Física, Cinvestav, A.P. 14-740, 07000 Ciudad de México, Mexico
[2]Instituto de Ciencias Nucleares, Universidad Nacional Autónoma de México, A.P. 70-543, 04510 Ciudad de México, Mexico
[3]Departamento de Óptica, Centro de investigación Científica y de Educación Superior de Ensenada, A.P. 360 Ensenada, BC 22860, Mexico
*david.bermudez@cinvestav.mx

Abstract: We experimentally observe the stimulated analogue of Hawking radiation produced in a photonic-crystal fiber, with a pulsed pump and a continuous-wave probe. In particular, we propose and demonstrate an innovative method to boost the efficiency and probe the coherence characteristics of the analogue Hawking effect relying on a double pump pulse with a controlled temporal delay. We show that the emitted analogue Hawking radiation corresponds to the coherently-added, interfering Hawking signals resulting from the probe interacting with each pump pulse. We introduce a simple effective Michelson interference model, and demonstrate excellent agreement between our experimental data and the predictions derived from this model. Importantly, while naively increasing the pump power in an attempt to boost the Hawking-radiation generation efficiency results in the distortion of the output signal, we show that at the maxima of the observed Hawking-signal interference pattern, the signal can be increased by a factor of >3 (up to 4 under ideal experimental conditions). This approach could be extended to the use of sequences of m pulses, resulting in a Hawking-signal enhancement of m^2.

1. Introduction

A new paradigm in optics involves fields that act themselves as optical elements to control light. Indeed, new phenomena occurring in optical fibers have been explored based on nonlinear interactions between solitons and other optical waves designed to reflect, trap, and control light by light. These systems include temporal interfaces and waveguides [1–3], solitonic cages and cavities [4,5], pulse trapping [6], emulation of Fabry-Perot and Bragg resonators [7], control of solitons using dispersive waves [8–10], manipulation of dark solitons [11], generation of frequencies via four-wave mixing [12], mixing of solitons and dispersive waves [13], as well as the emulation of event horizons [14,15].

In this paper, we concentrate on the so-called analogue Hawking effect, one of the known phenomena originating from the nonlinear interaction of light in a dielectric with third-order susceptibility. This effect represents a stimulated version of the optical analogue of the astrophysical Hawking radiation produced by the quantum vacuum in the vicinity of the event horizon of a black hole [16,17]. Initial experimental work in this direction involved interacting a continuous-wave (CW) probe with a pulsed pump [14,18]. The efficiency in such systems tends to be low since the fraction of the probe energy temporally overlapped with the pulsed pump is extremely small. In this context, recent work has exploited the interaction of a pulsed probe with a pulsed pump so as to drastically increase the efficiency of the nonlinear effects [15,19]. However, the experimental configurations with a CW probe are more straightforward than with a pulsed probe considering that no temporal synchronization is required.

#447201 https://doi.org/10.1364/OE.447201
Journal © 2022 Received 4 Nov 2021; revised 13 Jan 2022; accepted 25 Jan 2022; published 24 Feb 2022

Optics EXPRESS

While the use of an all-pulsed experimental scheme certainly has been successful [15], the much increased resulting experimental complexity motivated our search for ways to boost the efficiency in the technically simpler case of a CW probe. In this paper, we propose and demonstrate an innovative method to (1) boost the efficiency and (2) probe the coherence characteristics of the analogue Hawking effect based on a CW probe, as follows. As a first step, we set up our own version of a previous experiment to observe the frequency-shifting of a CW probe due to its interaction with a pulsed pump through the Kerr effect, which corresponds to the expected Hawking radiation analogue. As a second step, we propose and implement a novel experiment to demonstrate the use of a double pump pulse which leads to an interference effect in the Hawking signal, and translates into a four-fold increase in the conversion efficiency at interference maxima. Interestingly, this approach could be generalized to the use of sequences of more than two pump pulses for an even greater increase in the conversion efficiency, with an enhancement factor which scales as the square of the number of pulses. Furthermore, this approach shows that the emitted radiation is coherent, since otherwise interference would not occur between two separate sources, as we in fact demonstrate. Such coherence represents an expected property of the true (astrophysical) Hawking radiation seeded by the quantum vacuum. So as to fully understand the measured spectra, we present a theoretical model based on an effective Michelson interferometer in which, instead of relying on physical mirrors, the probe is reflected from light itself at each of the two pump pulses. We believe that this work provides an interesting new tool for further experimental studies of the analogue Hawking effect.

2. Nonlinear optical model for the analogue Hawking effect

The first necessary ingredient in our experiment is an intense ultra-short pump pulse traveling in a third-order dielectric medium. Due to the optical Kerr effect, the high-intensity electric field leads to a slight increase in the refractive index of the medium. In our case, the pulse propagates through an optical fiber so that the original refractive index n_0 increases by $\delta n \propto I(z,t)$, where I is the pulse intensity. This effect can be understood in terms of an effective moving medium.

The second ingredient is a probe wave to interact with the effective moving medium. For this purpose, the probe should have a very similar group velocity to the pump pulse, so that the change of refractive index caused by the pump pulse is sufficient to reverse the propagation direction of the probe relative to the pump: this is the regime known as extreme nonlinear optics (XNLO) [20–22]. Particularly, in our experimental work we focus on a case in which the probe is initially faster and thus reaches the pump pulse, slowing down in the process until it matches the pump velocity. This represents an unstable state for the probe: it can either traverse the pump while retaining its original frequency or continue to slow down and blueshift to a new frequency. The blueshifted signal traveling more slowly than the pump constitutes the optical analogue of the Hawking radiation [14,15]. The conversion efficiency can be calculated as the ratio between the intensities of the blueshifted Hawking signal and the incoming probe.

Our nonlinear medium should fulfill two conditions: have a sufficiently large nonlinearity and satisfy the mentioned quasi group-velocity matching between two different frequencies (the pump and the probe) [23]. The fulfilment of these conditions is possible in highly-nonlinear fibers, particularly in photonic-crystal fibers (PCFs). These fibers exhibit a region of anomalous dispersion such that the group index presents both a local minimum and a maximum, instead of decreasing monotonically with wavelength as is common for fused silica optical fibers [24].

A simple and effective means to study wave propagation in a single-mode fiber is the nonlinear Schrödinger equation (NLSE) [25], which is the approach we use to model the analogue Hawking effect. Note that while the derivation of the NLSE relies on several approximations and has been surpassed in numerical solutions by other equations requiring fewer approximations, it is still widely used because it provides valuable physical intuition [18,26].

Optics EXPRESS

In our analysis, we use the so-called pump-probe approximation, in which the pump is considered static, and the main focus is to analyze its effect on the probe [27]. This approximation is valid if the pump is much more intense than the probe, as is our case. By transforming the laboratory coordinates to a frame of reference co-moving with the pump, the NLSE transforms into a standard Schrödinger equation for the probe, with an effective potential proportional to the intensity of the pump. The Hawking signal produced by the interaction in the pump-probe regime is more easily studied in the co-moving pulse frame [14]. This theoretical approach has resulted in excellent agreement with the experiment in terms of the frequency and efficiency of the resulting Hawking signal [18]. The frequency of the resulting analogue Hawking can be calculated through the conservation of the co-moving probe frequency upon its conversion process [28].

In the co-moving frame, the probe is slowed down by the pump until it comes to a complete standstill at a certain point (referred to as the white-hole horizon) defined by its intensity, at which it can be either transmitted or reflected, in both cases maintaining its co-moving frequency (Fig. 1):

$$\omega'(\omega) = \gamma\left(1 - \frac{n(\omega)u}{c}\right)\omega, \tag{1}$$

where u is the pump group velocity, γ is the Lorentz factor of u, and ω is the frequency in the laboratory frame.

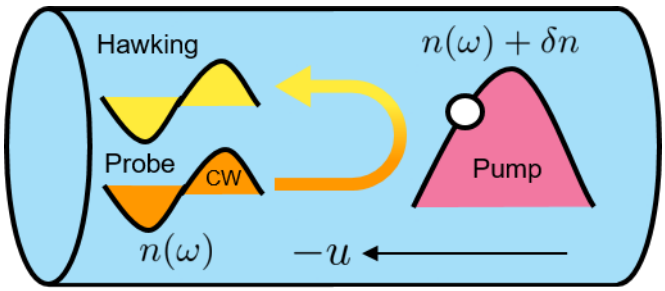

Fig. 1. In the laboratory frame, an intense pump pulse (red) travels along a fiber inducing a refractive index increment due to the Kerr effect. A continuous wave probe (orange) approaches the pump pulse and is slowed down and frequency-shifted by the pulse. The resulting signal constitutes the analogue Hawking radiation (yellow). In the co-moving frame, the CW approaches the stationary pump and is reflected at a certain intensity, the analogue of a white-hole horizon (white circle). The co-moving frequency is conserved in this process.

Due to the dispersive nature of the optical analogues, the horizon is best defined by its frequency and not by a spatial location, as in astrophysics. The horizon frequency has the same group velocity as the pump, i.e., $d\omega'/d\omega = 0$. The factor $d\omega'/d\omega$ defines the velocity in the co-moving frame: faster [slower] waves have a positive [negative] derivative. The dispersion relation of our fiber is presented in Fig. 2 in the form of the co-moving frequency $\omega'(\omega)$. The probe frequency ω_p (orange) is slightly lower than the horizon frequency ω_h (black) and upon its interaction with the pump pulse, it can be shifted to the Hawking frequency ω_{HR} (yellow) which is higher than the horizon frequency.

Optics EXPRESS

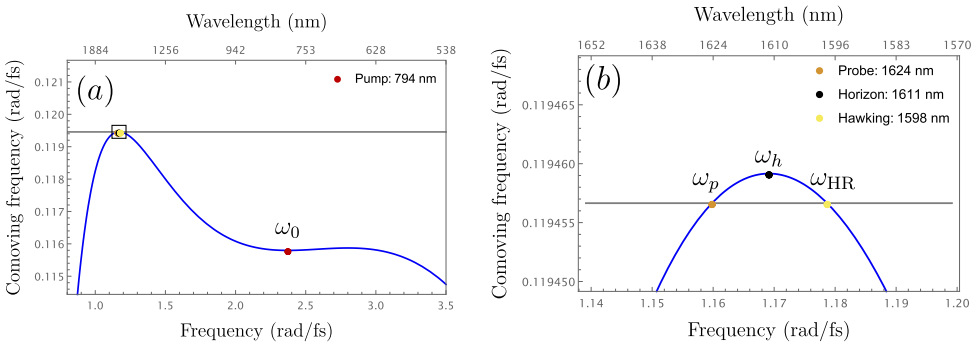

Fig. 2. The dispersion relation of the fiber is represented by the co-moving frequency as a function of the laboratory frequency $\omega'(\omega)$, for a wide spectral window (a) and for the specific region of interest (b). Note that the resulting Hawking radiation is blueshifted from the incoming probe (as this is a white-hole horizon).

3. Measuring the analogue Hawking signal

Detailed knowledge of the PCF dispersion relation is crucial for the design and interpretation of our experiment. We obtain the fiber dispersion relation through the following procedure: (1) we map the transverse fiber geometry through a scanning electron microscope, (2) we simulate a catalog of thousands of dispersion relations stemming from similar geometries using the FemSIM Mode Solver, (3) in a related experiment (not discussed here, see Ref. [29] for details), we spectrally resolve the photon pairs generated by the spontaneous four-wave mixing process, and (4) we find the dispersion relation that best fits our measurements. Having determined the dispersion relation, we predict the Hawking frequency for a given probe frequency ω_p by solving $\omega'(\omega) = \omega'(\omega_p)$ for ω (Fig. 2).

Figure 3 shows our experimental setup. The beam from a Ti:sapphire pulsed laser with a temporal duration of around 110 fs, tunable in the range 780-810 nm, and with a repetition rate of 83 MHz, is sent to a power and delay controller, with the purpose of preparing double pulses to constitute the pump in the analogue Hawking process. A half-wave plate (HWP1) and polarizer (POL1) are used to control the pump power, which is subsequently split by a polarized beam-splitter (PBS), with the power in each arm controlled by a second half-wave plate (HWP2) preceding the PBS. Both the reflected, vertically-polarized arm and the transmitted, horizontally-polarized arm include a quarter-wave plate (QWP1, QWP2) followed by a mirror such that the polarization is reversed on the return trip to the PBS. This ensures that all light exits the PBS through its fourth port, thus forming a Michelson interferometer. Mounting one of the interferometer end-mirrors on a computer-controlled linear motor enables us to produce two-pulse sequences with a controllable temporal delay. Note that one of the two arms may be blocked so as to obtain single pulses instead of pulse pairs when needed. A second polarizer at the interferometer output is set to transmit the 45° polarization, ensuring that the two transmitted pulses are co-polarized (although with a power reduction by a factor of 2). A third half-wave plate (HWP3) is used to align the polarization of the pump pulse pair to the desired axis of the optical fiber to produce the Hawking effect.

A dichroic mirror (DM1; designed to transmit wavelengths λ>900 nm, while reflecting other wavelengths) allows us to combine into a single spatial mode the pump (in the form of a two-pulse sequence) with the probe, formed by the beam from a CW laser. Specifically, we use a narrowband, fiber-output CW laser, tunable between 1533 to 1633 nm (Keysight B1949A), with its beam transmitted through a polarizer (POL3) to ensure that the probe polarization remains

Optics EXPRESS

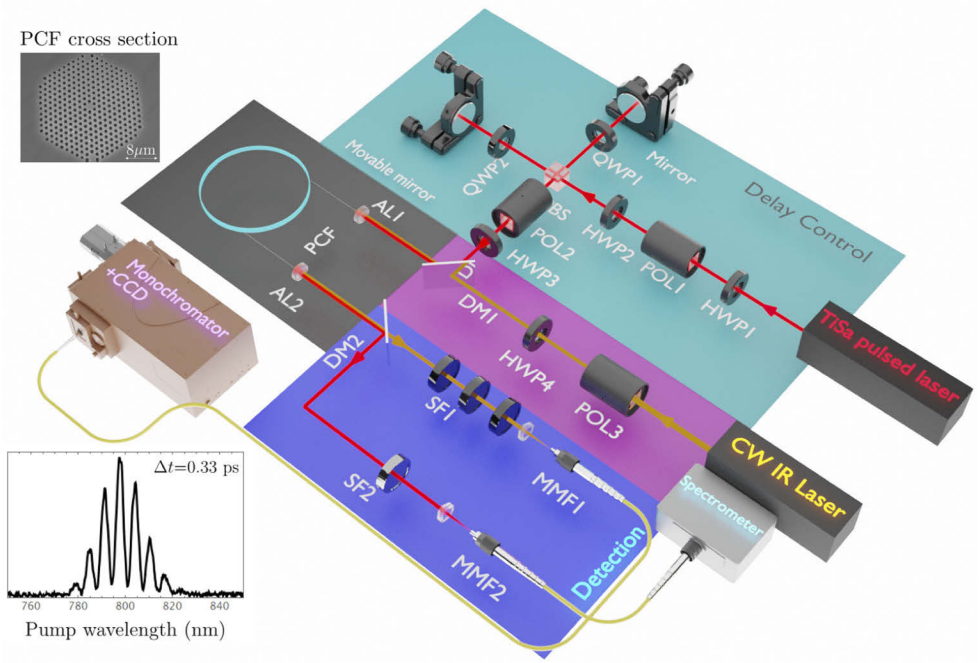

Fig. 3. Experimental setup. For clarity, we divide it into three sections: delay and power control for the Ti:sapphire pulsed laser (light blue area), polarization control for the CW long-infrared laser (pink), and detection (purple). The MMF1 leads to a monochromator fitted with an InGaAs camera (Andor Idus) at its output, while the MMF2 leads to a compact spectrometer (Ocean Optics USB-4000). The movable mirror is initially blocked to measure the frequency shift with a single pulse. The two insets show the cross section of the used PCF and the pump spectra for a non-zero temporal delay.

stable, followed by a half-wave plate (HWP4) used to align the probe polarization to the desired axis of the optical fiber.

The combined pump-probe mode is coupled with the help of an aspheric lens (AL1) into a 1 m length of photonic-crystal fiber (NKTPhotonics NL-PM-750). Light emanating from the fiber is collimated using a second aspheric lens (AL2). A second dichroic mirror (DM2; designed to transmit wavelengths λ>925 nm, while reflecting other wavelengths) thus defines an IR (transmitted) arm containing the probe, along with the Hawking signal, and a visible (reflected) arm containing the pump pulse pair. Light in the IR detection arm is transmitted through a filter assembly (SF1) composed of a longpass filter (designed to transmit wavelengths λ>980 nm), followed by a 1600 ± 6 nm bandpass filter. Detection on this arm is accomplished by a grating-based monochromator (Andor SR-500i), fitted with a linear InGaAs CCD detection array (iDus InGaAs 1.7 DU490A) at its output. Light in the visible detection arm is transmitted through a bandpass filter (SF2) centered at 795 nm with a 150 nm bandwidth. Detection in this arm is accomplished by a compact grating-based spectrometer (Ocean Optics USB-4000).

As a first experimental test, we measure the Hawking radiation produced by a single pump pulse; for this purpose we block the translatable-mirror Michelson arm. We carry out the experiment aligning both the pump and probe first to the slow axis and then to the fast axis of the PCF. We use a pump at 791 nm with a power of 0.95 mW (measured at the fiber exit), with the corresponding horizon frequency at 1610.8 nm. We couple ~150 μW of probe power to the fiber and measure the frequency shift for both fiber axes. The results are shown in Fig. 4(a), where the solid lines represent the theoretical predictions and the points the experimental data.

Optics EXPRESS

In Fig. 4(b), the points represent the calculated conversion efficiency from the measurements (ratio between the Hawking signal to the coupled infrared signal), the dashed lines are Gaussian fits, and the solid lines are obtained from the theoretical model in Ref. [18]. The discrepancy between experimental and theoretical efficiency values can be attributed to various experimental imperfections. Note that in our ensuing experiments we use the slow axis because of the larger efficiencies attainable in comparison to the fast axis.

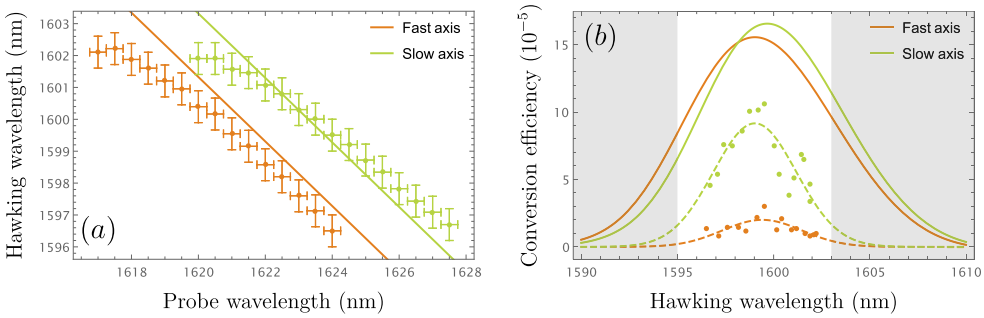

Fig. 4. Wavelength (a) and efficiency (b) of the measured Hawking signal for a single pump pulse for both principal axes of the PCF using a pump at 791 nm with 0.95 mW power. The points represent our measurements while the solid lines represent theory curves. Gray regions indicate spectral areas that cannot be observed experimentally (see text). Dashed lines in (b) correspond to a Gaussian fit of the data points.

The main challenge that we face when using a CW probe is the low resulting analogue Hawking efficiency. A simple strategy to boost the Hawking signal is to increase the pump power. However, this quickly results in a complete deformation of the Hawking signal, as a consequence of other nonlinear effects occurring during the pump propagation in the fiber, such as soliton fission, Raman effect, and supercontinuum generation [30]. So as to avoid these complications, we propose and demonstrate a novel strategy to boost the Hawking signal based on the use of a pump in the form of a pulse pair with a controlled temporal delay.

4. Boosting the Hawking signal through interference

The two arms in the Michelson interferometer allow us to produce a pump pulse pair with a controlled temporal delay, exhibiting a spectrum with oscillations as shown in the inset in Fig. 3. In our experiments we align both the visible pump and the IR probe to the slow axis of the fiber. As a starting point, we set the position of the translatable mirror 1 mm away from the zero-delay setting (corresponding to a delay of 6.6 ps), and proceed to take data of the IR spectrum with the help of the monochromator, for both pump configurations of interest: single- and double-pulse. The experimental results are shown in Fig. 5(a), which displays the Hawking-signal spectrum resulting from a single-pulse pump (green curve), and from a double-pulse pump (black curve) with a delay of 6.6 ps. It becomes clear that whereas the single-pulse case leads to a Hawking signal in the form of a single spectral peak (with a width of $\sim$ 5 nm), the double-pulse case leads to a spectrum which includes an interference pattern. Importantly, the interference pattern yields intensity maxima that are higher than the single-pulse signal by a factor >3 (note that, as has been mentioned, the calculations show that a factor of 4 is possible under ideal conditions). In Fig. 5(b) we show the wavelength λ_{HR} at which the maximum intensity occurs in the Hawking signal for the single- and double-pulse cases (calculated from Gaussian fits of the spectrum, in the single-pulse case, and of the envelope of the spectrum, in the double-pulse case). The fact that λ_{HR} is essentially the same for the single- and double-pulse cases, indicates that the interference-mediated enhancement in the Hawking signal is obtained without the appearance of

Optics EXPRESS

additional nonlinear effects, as can occur by simply increasing the pump power in an attempt to boost the Hawking signal.

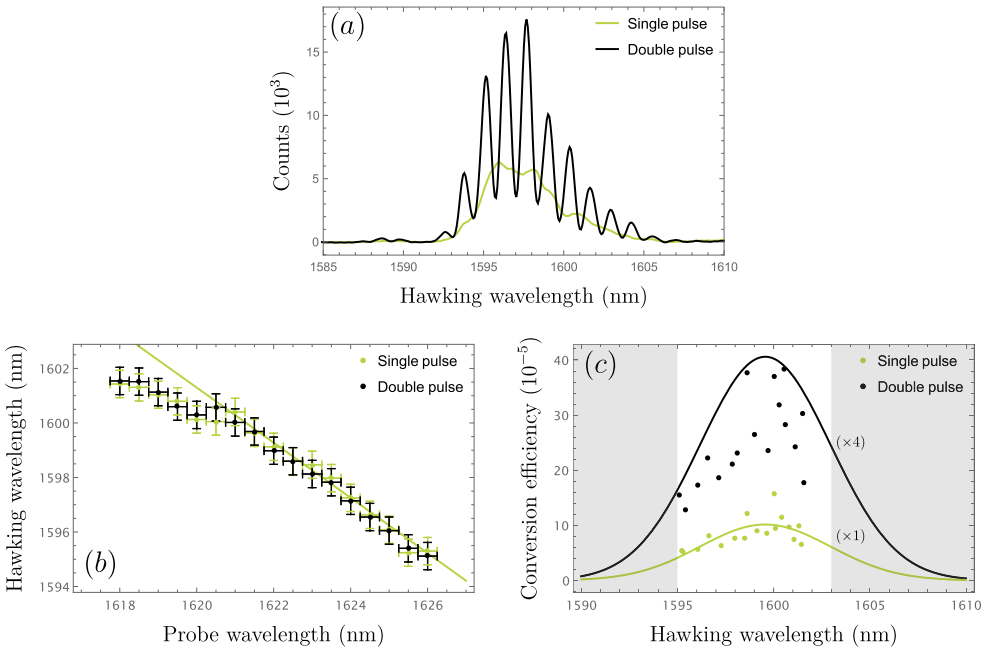

Fig. 5. Measured analogue Hawking radiation signal: Example spectra for a 1623.5 nm probe in the single- and double-pulse pump cases (a), probe wavelength dependence (b) and efficiency (c) of the Hawking signal in the single-pulse (green) and double-pulse (black) cases, using a 796.5 nm at 0.95 mW pump and a temporal delay of 6.6 ps. The green line in (c) represents a Gaussian fit of the single-pulse data-points, and the black line corresponds to the ideal enhancement of this signal by a factor of 4.

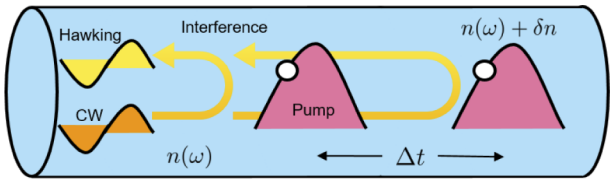

Fig. 6. The CW probe interacts with the two pump pulses separated by a delay Δt. In the co-moving frame, the Hawking signals produced at the two pulses can be regarded as probe reflections from the pump pulses. This leads to an effective Michelson interference model in which the two interferometer arms correspond to the two probe reflections.

We compute the Hawking efficiency for each data point in Fig. 5(b) for both in the single- and double-pulse cases. The results are plotted in Fig. 5(c). Note that while the gray band on the left indicates that no data is displayed because it lies outside of the spectral transmission window of the bandpass filter in SPF1, and the gray band on the right indicates that no data is displayed because the probe and Hawking signals become too close to each other. The green curve shows a Gaussian fit of the single-pulse pump conversion efficiency (green points), and the black curve represents the ideal pulse-pair conversion efficiency resulting from multiplying the single-pulse values by a factor of 4. Note that, although the two-pulse data points (black) fall short of the theoretical four-fold enhancement, they do show a remarkable enhancement.

Optics EXPRESS

5. Reinterpreting the Hawking signal as Michelson interference

The condition for the analogue Hawking effect to occur is that the probe frequency is close enough to the horizon frequency to allow for the Kerr effect of the pump pulse to bring it to a halt it in the co-moving frame. The expected Hawking frequency can be calculated by matching the probe and Hawking frequencies in the co-moving frame

$$\omega'_{\mathrm{HR}} = \omega'_p, \tag{2}$$

which in turn leads to the following relationship between the probe and the Hawking group velocities v'_p and v'_{HR}, in the co-moving frame

$$v'_{\mathrm{HR}} \approx -v'_p. \tag{3}$$

Thus, remarkably, in the co-moving frame the Hawking signal may be regarded as the reflection of the probe from the pump pulse. Because in our case the pump is in the form of a sequence of two pulses, each pump pulse may independently result in a Hawking signal, with the overall Hawking signal then given by the coherent addition of the two signals (Fig. 6). This behavior may be understood in terms of an effective Michelson interferometer for the analogue Hawking radiation produced with each of the two interferometer arms corresponding to the Hawking signals produced by the probe interacting with each of the two pump pulses. Note that the temporal delay between the two interferometer arms may be controlled through the pump-pulse delay. It is important to note that this effective Michelson interferometer acting on the analogue Hawking radiation and defined by light is distinct from the Michelson interferometer acting on the pump pulses to yield the pulse pair.

In order to test this effective-Michelson interpretation, let us write a simple model for the overall Hawking signal, involving the coherent addition of two independent Hawking signals, each described by a Gaussian temporal profile, as follows

$$E(t) \propto \exp\left[-\left(\frac{t}{\sigma_t}\right)^2 + i\omega_{\mathrm{HR}}t\right] + \exp\left[-\left(\frac{t-\Delta t}{\sigma_t}\right)^2 + i\omega_{\mathrm{HR}}(t-\Delta t) + i\omega_p\Delta t\right]. \tag{4}$$

In Eq. (4), σ_t is the temporal duration of each of the two Gaussian-shaped Hawking signals, Δt is the pump-pulse delay, ω_{HR} is the Hawking frequency, and ω_p is the probe frequency. Note in Fig. 6 that the phase difference between the two effective Michelson arms includes: (1) the phase $\omega_p\Delta t$ accumulated by the portion of the probe transmitted by the first pulse that reaches the second pulse, and (2) the phase $\omega_{\mathrm{HR}}\Delta t$ accumulated by the Hawking radiation produced by the second pulse that propagates back to the first pulse.

The spectral intensity $I(\omega;\Delta t)$ can then be calculated as $|\tilde{E}(\omega)|^2$, where $\tilde{E}(\omega)$ represents the Fourier transform of $E(t)$, obtaining

$$I(\omega;\Delta t) \propto \exp\left[-\frac{\sigma_t^2}{2}(\omega-\omega_{\mathrm{HR}})^2\right]\left\{1+\cos[\Delta t(\omega-\omega_p)]\right\}. \tag{5}$$

In our experiment we record the spectrum of the Hawking signal for 400 equally-spaced delay configurations, ranging from −1 mm (or −6.6 ps) to 1 mm (or 6.6 ps). We set the probe to 1624 nm, with a power of 150 μW, while the pump is centered at 794 nm with a power of 1.52 mW (measured at the fiber exit, which is distributed equally among the two interferometer arms), resulting in a Hawking frequency of 1598 nm.

The resulting experimental data is shown in Fig. 7(a), and the corresponding plot of $I(\omega;\Delta t)$ according to the model in Eq. (5) is shown in panel (d). It may be seen that (apart from the region near $\Delta t = 0$) there is an excellent agreement between the experimental and modelled behaviors. In

Optics EXPRESS

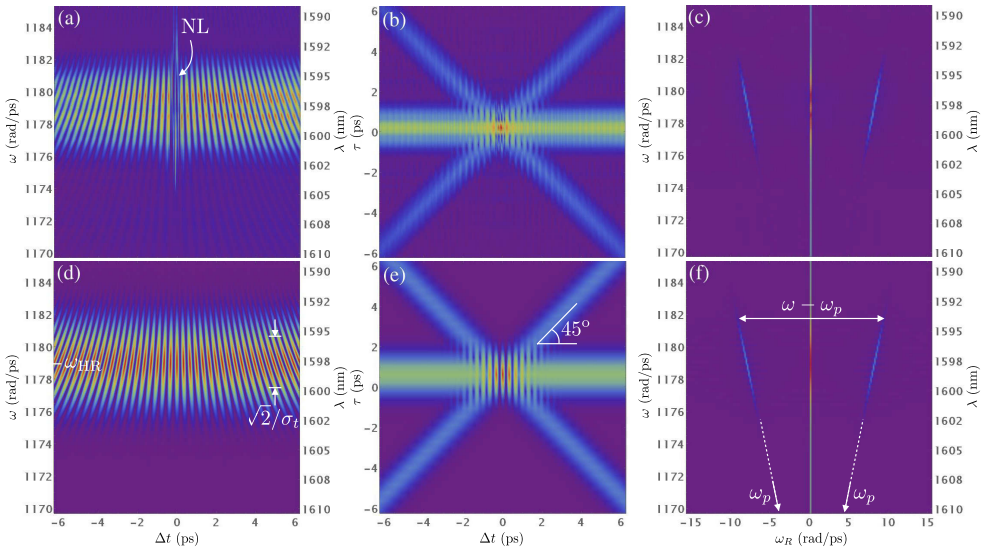

Fig. 7. Interference spectra of analogue Hawking radiation for a range of temporal delay configurations (a,d). Fourier transform of interference spectra at each temporal delay value (b,e). Fourier transform of the Hawking-signal for each frequency ω (the reference frequency ω_R variable is conjugate to Δt) (c,f). Note that while the top row corresponds to experimental data [direct in (a) and processed in (b) and (c)], the bottom row corresponds to our model.

plotting $I(\omega;\Delta t)$ we have used as parameters the known probe ω_p and Hawking ω_{HR} frequencies. In addition, from a Gaussian fit of the pump spectrum (in the single pulse configuration) we can obtain the spectral width $\sqrt{2}/\sigma_t$, from which the temporal width is calculated.

As a second comparison exercise, we also show the result of Fourier transforming the spectrum at each delay value Δt, yielding the auto-correlation function of the emitted Hawking radiation (in accordance with the Wiener-Khintchine theorem [31]). When displaying the result of applying such a transformation to the experimental data at all delay values, one obtains a two dimensional function of two temporal variables: τ that corresponds to the Fourier conjugate variable to ω, and the pump-pulse temporal delay Δt, as shown in Fig. 7(b). Applying the same transformation to the modelled spectral intensity $I(\omega;\Delta t)$ we obtain the result shown in panel (c). Apart from the fact that there is clearly an excellent agreement between (b) and (e), it is also noteworthy that the $\pm$ unit slope of the two diagonal stripes in panel (b) indicates that the pump-pulse delay acts as expected.

As a third comparison exercise, we show the result of Fourier transforming the experimental data for each constant Hawking frequency ω, thus obtaining a plot with a relative frequency variable ω_R (Fourier conjugate variable to Δt) in the horizontal axis and ω in the vertical axis. While in Fig. 7(c) we show the effect of applying such a Fourier transform to the experimental data in (a), in (f) we show the effect of applying it the modelled behavior in (d). In both cases, we obtain a central vertical stripe surrounded by two diagonal stripes which approach each other for lower frequencies ω. Additionally, as a useful self-consistency test, if one extrapolates the two diagonal stripes, one can check that they meet at $\omega = \omega_p$, as the model predicts.

Considering the excellent agreement between the experimental and modelled behaviors in each of the three columns of Fig. 7, we conclude that the signal produced in the experiment indeed corresponds to the coherently-added, interfering Hawking signals, which can be regarded as probe reflections from the two pump pulses. Our interferometric approach clearly shows that the emitted radiation is coherent, since otherwise interference would not occur between two separate

Optics EXPRESS

sources, as we in fact demonstrate. Our experiment represents the first experimental verification of this coherence property for stimulated Hawking radiation in the optical context. This property is also expected for the true (astrophysical) Hawking radiation seeded by the quantum vacuum.

Note that the discrepancy between the experiment and the model [see Fig. 7(a) and (d)] around zero delay ($\Delta t = 0$) is related to the fact that in this region the two pump pulses overlap yielding a single peak with twice the intensity, which produces undesired higher-order nonlinear effects as it propagates through the fiber, region marked as NL in panel (a). Indeed, it was mentioned above that naively increasing the pump power leads to distortion of the Hawking signal. Note also that because our fiber is not long enough to allow multiple reflections of the Hawking signal, as indicated by our calculations inspired by Ref. [4] (not shown here), the Michelson interference model used here is more appropriate than one based on Fabry-Perot interference.

6. Conclusions

We report an experiment based on a photonic-crystal fiber in which a continuous wave optical signal interacts with a pulsed pump, generating a stimulated analogue Hawking signal, blueshifted from the white-hole analogue of the probe. Knowledge of the fiber dispersion obtained from an independent characterization of the fiber through spontaneous four-wave mixing, allows us to predict the wavelength of the Hawking signal leading to excellent agreement with the experiment.

We discuss that the observed Hawking signal may be regarded (in a frame of reference co-moving with the pump) as the reflection of the probe from the pump pulse. In this paper, we introduce the use of a double pump pulse, with a controlled temporal delay, and show that the Hawking signal produced then corresponds to the coherent addition of the independent signals from the two pump pulses, as evidenced by the interference pattern observed in the outgoing Hawking spectrum. We have thus verified for the first time this coherence property in the stimulated optical context.

From a purely optical perspective, the implementation of a Michelson interferometer defined by light pulses in a dielectric rather than by physical mirrors is novel. This phenomenon is correctly explained by our model given by Eqs. (4) and 5 in the frame comoving with the pump pulses. Our work expands the existing catalogue of experiments that control light-by-light and, to the best of our knowledge, is the first interferometer defined by light. This technique could be used to enhance the efficiency and visibility of different nonlinear effects—not only analogue Hawking radiation—while controlling unwanted signals.

Importantly, while naively increasing the pump power in an attempt to boost the analogue Hawking generation efficiency leads to distortion of the signal produced, we show that at the interference maxima, the Hawking signal is boosted by a factor >3 (which can be as high as 4 under ideal conditions). We introduce a simple model of the analogue Hawking radiation produced by an effective Michelson interferometer, and show that there is an excellent agreement between our experimentally-obtained Hawking spectra for a range of temporal delay values and the predictions derived from this model.

We point out that our pulse pair approach could be generalized to sequences of m pulses, which would result, importantly, in an m^2 enhancement in the Hawking signal. This enhancement could help in the eventual detection of the spontaneous version of the Hawking radiation optical analogue, where no probe is used and the quantum vacuum seeds the effect. We believe that our current work on the one hand will facilitate future research on optical analogues of Hawking radiation, and on the other hand may present new avenues for purely optical experiments on the control of light by light.

Funding. Consejo Nacional de Ciencia y Tecnología (CF-2019-217559, CF-2019-51458, PhD-456558); Universidad Nacional Autónoma de México (IN103521); Air Force Office of Scientific Research (FA9550-21-1-0147); Centro de Investigación Científica y de Educación Superior de Ensenada, Baja California (F0F144).

Optics EXPRESS

Acknowledgments. R.F.-E. and D.B acknowledge the support by Conacyt (Mexico) grant CF-2019-51458. A.U. acknowledges support from PAPIIT (UNAM) grant IN103521, from Conacyt grant CF-2019-217559, and from AFOSR grant FA9550-21-1-0147. K. G.-P. acknowledges the support from CICESE grant F0F144. R.F.-E. acknowledges the support from Conacyt PhD-scholarship 456558.

The authors would like to thank the support from Roberto Ramírez-Alarcón. R.F.-E. would like to thank the staff of the Experimental Quantum Optics Group at ICN-UNAM for their technical and emotional support in these difficult times. In particular to Omar Calderon-Losada, Mayte Y. Li-Gomez, and Samuel Corona-Aquino for the enriching discussions and to Erasto Ortiz-Ricardo and Cesar Bertoni-Ocampo for their comments and technical help.

Disclosures. The authors declare no conflicts of interest.

Data Availability. Data underlying the results presented in this paper are not publicly available at this time but may be obtained from the authors upon reasonable request.

References

1. B. W. Plansinis, W. R. Donaldson, and G. P. Agrawal, "What is the temporal analog of reflection and refraction of optical beams?" Phys. Rev. Lett. **115**(18), 183901 (2015).
2. B. W. Plansinis, W. R. Donaldson, and G. P. Agrawal, "Temporal waveguides for optical pulses," J. Opt. Soc. Am. B **33**(6), 1112 (2016).
3. B. W. Plansinis, W. R. Donaldson, and G. P. Agrawal, "Spectral splitting of optical pulses inside a dispersive medium at a temporal boundary," J. Opt. Soc. Am. B **52**(12), 1–8 (2016).
4. S. F. Wang, A. Mussot, M. Conforti, X. L. Zeng, and A. Kudlinski, "Bouncing of a dispersive wave in a solitonic cage," Opt. Lett. **40**(14), 3320 (2015).
5. R. Driben, A. V. Yulin, A. Efimov, and B. A. Malomed, "Trapping of light in solitonic cavities and its role in the supercontinuum generation," Opt. Express **21**(16), 19091 (2013).
6. S. Hill, C. E. Kuklewicz, U. Leonhardt, and F. König, "Evolution of light trapped by a soliton in a microstructured fiber," Opt. Express **17**(16), 13588–13601 (2009).
7. T. Voytova, I. Oreshnikov, A. V. Yulin, and R. Driben, "Emulation of Fabry–Perot and Bragg resonators with temporal optical solitons," Opt. Lett. **41**(11), 2442 (2016).
8. L. Tartara, "Soliton control by a weak dispersive pulse," J. Opt. Soc. Am. B **32**(3), 395 (2015).
9. J. Gu, H. Guo, S. Wang, and X. Zeng, "Probe-controlled soliton frequency shift in the regime of optical event horizon," Opt. Express **23**(17), 22285 (2015).
10. Z. Deng, J. Liu, X. Huang, C. Zhao, and X. Wang, "Active control of adiabatic soliton fission by external dispersive wave at optical event horizon," Opt. Express **25**(23), 28556 (2017).
11. Z. Deng, J. Liu, X. Huang, C. Zhao, and X. Wang, "Dark solitons manipulation using optical event horizon," Opt. Express **26**(13), 16535 (2018).
12. C. Mas Arabí, F. Bessin, A. Kudlinski, A. Mussot, D. Skryabin, and M. Conforti, "Efficiency of four-wave mixing between orthogonally polarized linear waves and solitons in a birefringent fiber," Phys. Rev. A **94**(6), 063847 (2016).
13. D. V. Skryabin and A. V. Yulin, "Theory of generation of new frequencies by mixing of solitons and dispersive waves in optical fibers," Phys. Rev. E **72**(1), 016619 (2005).
14. T. G. Philbin, C. Kuklewicz, S. Robertson, S. Hill, F. König, and U. Leonhardt, "Fiber-optical analog of the event horizon," Science **319**(5868), 1367–1370 (2008).
15. J. Drori, Y. Rosenberg, D. Bermudez, Y. Silberberg, and U. Leonhardt, "Observation of stimulated Hawking radiation in an optical analogue," Phys. Rev. Lett. **122**(1), 010404 (2019).
16. W. G. Unruh, "Experimental black-hole evaporation?" Phys. Rev. Lett. **46**(21), 1351–1353 (1981).
17. C. Barceló, S. Liberati, and M. Visser, "Analogue gravity," Living Rev. Relativ. **14**(1), 3 (2011).
18. A. Choudhary and F. König, "Efficient frequency shifting of dispersive waves at solitons," Opt. Express **20**(5), 5538–5546 (2012).
19. L. Tartara, "Frequency shifting of femtosecond pulses by reflection at solitons," IEEE J. Quantum Electron. **48**(11), 1439–1442 (2012).
20. T. K. Allison, A. Cingöz, D. C. Yost, and J. Ye, "Extreme nonlinear optics in a femtosecond enhancement cavity," Phys. Rev. Lett. **107**(18), 183903 (2011).
21. Y. Rosenberg, "Optical analogues of black-hole horizons," Phil. Trans. R. Soc. A. **378**(2177), 20190232 (2020).
22. M. Wegener, *Extreme Nonlinear Optics: An Introduction*, Advanced Texts in Physics (Springer, 2005).
23. K. E. Webb, M. Erkintalo, Y. Xu, N. G. R. Broderick, J. M. Dudley, G. Genty, and S. G. Murdoch, "Nonlinear optics of fibre event horizons," Nat. Commun. **5**(1), 4969 (2014).
24. M. N. Polyanskiy, "Refractive index database," https://refractiveindex.info. Accessed: 2010-08-30.
25. G. Agrawal, *Nonlinear Fiber Optics*, Optics and Photonics (Elsevier Science, 2013).
26. A. Moreno-Ruiz and D. Bermudez, "Hawking temperature in dispersive media: Analytics and numerics," Ann. Phys. **420**, 168268 (2020).
27. J. D. Rincon-Estrada and D. Bermudez, "Instabilities in an optical black-hole laser," Ann. Phys. **533**(1), 2000239 (2021).
28. S. Robertson and U. Leonhardt, "Frequency shifting at fiber-optical event horizons: The effect of raman deceleration," Phys. Rev. A **81**(6), 063835 (2010).

Optics EXPRESS

29. D. D. la Torre-Robles, F. Dominguez-Serna, G. L. Osorio, A. B. U'Ren, D. Bermudez, and K. Garay-Palmett, "Frequency and polarization emission properties of a photon-pair source based on a photonic crystal fiber," Sci. Rep. **11**(1), 18092 (2021).
30. J. M. Dudley, G. Genty, and S. Coen, "Supercontinuum generation in photonic crystal fiber," Rev. Mod. Phys. **78**(4), 1135–1184 (2006).
31. E. Steward, *Fourier Optics: An Introduction* (2 Edition), Dover Books on Physics Series (Dover Publications, Incorporated, 2012).